scientific reports

Check for updates

OPEN

Saccades influence functional modularity in the human cortical vision network

George Tomou[1,2,3,4,7], Bianca R. Baltaretu[1,2,3,5,6,7], Amirhossein Ghaderi[1,2,3,8] & J. Douglas Crawford[1,2,3,4,5,8]✉

Visual cortex is thought to show both dorsoventral and hemispheric modularity, but it is not known if the same functional modules emerge spontaneously from an unsupervised network analysis, or how they interact when saccades necessitate increased sharing of spatial information. Here, we address these issues by applying graph theory analysis to fMRI data obtained while human participants decided whether an object's shape or orientation changed, with or without an intervening saccade across the object. BOLD activation from 50 vision-related cortical nodes was used to identify local and global network properties. Modularity analysis revealed three sub-networks during fixation: a bilateral parietofrontal network linking areas implicated in visuospatial processing and two lateralized occipitotemporal networks linking areas implicated in object feature processing. When horizontal saccades required visual comparisons between visual hemifields, functional interconnectivity and information transfer increased, and the two lateralized ventral modules became functionally integrated into a single bilateral sub-network. This network included 'between module' connectivity hubs in lateral intraparietal cortex and dorsomedial occipital areas previously implicated in transsaccadic integration. These results provide support for functional modularity in the visual system and show that the hemispheric sub-networks are modified and functionally integrated during saccades.

Keywords Cerebral cortex, Visual features, Saccades, Transsaccadic integration, Functional magnetic resonance imaging, Graph theory analysis, Modularity

Vision supports various perceptual, cognitive, and sensorimotor processes by influencing signals throughout the cerebral cortex. Given the complexity and broad distribution of these signals, the visual system is often described in terms of *functional modularity*, i.e., divisions based on *hemispheric lateralization* of the visual fields[1,2] and *dorsoventral streams* for fundamentally different computations[3,4]. These concepts are largely based on traditional region-based neurpsychological and neuroimaging approaches. This begs two questions: 1) does the cortical distribution of visual signals show the same modularity, and how are these signals communicated in tasks that require the integration of multiple modules? For example, in the presence of saccadic eye movements, the visual system is thought to engage both the dorsal and ventral streams[5] and often requires the remapping and sharing of information across visual fields[6,7].

Anatomic and functional lateralization was one of the first properties discovered in the visual system and is now widely assumed as fact, at least early in the system. Anatomic projections from the thalamus to early visual cortex promote a clear contralateral visual field specificity in occipital cortex[1,8]. However, visual-field specificity is less clear at higher levels of brain function. For example, parietal cortex shows a propensity to code contralateral visual field in neuroimaging studies[6,8] but parietal field specificity is less clear in neurophysiological signals and visuomotor deficits[9].

Dorsoventral modularity was originally based on neurophysiological recordings in primates: Ungerleider and Mishkin[4] proposed that the feedforward processing of vision is divided into a ventral (occipital-temporal) 'what' stream versus a dorsal (occipital-parietal) 'where' stream for vision. Goodale and Milner[3,10–12] later argued that the better distinction is 'what' versus 'how', where the ventral stream is used for perception and the dorsal

[1]Centre for Vision Research, York University, Room 0009A, Lassonde Bldg, Toronto, ON M3J 1P3, Canada. [2]Centre for Integrative and Applied Neuroscience, York University, Toronto, Canada. [3]Vision: Science to Applications (VISTA) program, York University, Toronto, Canada. [4]Department of Psychology, York University, Toronto, Canada. [5]Department of Biology, York University, Toronto, Canada. [6]Department of Experimental Psychology, Justus Liebig University Giessen, Giessen, Germany. [7]George Tomou and Bianca R. Baltaretu contributed equally to this work. [8]Amirhossein Ghaderi and Douglas Crawford jointly supervised this work. ✉email: jdc@yorku.ca

stream is used for action. Subsequent neuroimaging studies have supported the division of object recognition in ventrolateral occipital and temporal cortex[13,14] as opposed to saccade and reach areas in posterior parietal cortex[15–17]. Dorsal stream areas like the parietal eye fields are closely associated with prefrontal areas, including the frontal eye fields, supplementary eye fields, and dorsolateral prefrontal cortex. Collectively, the latter areas form both the cortical saccade network[18–20] and the 'dorsal attention network', exerting top-down influences on visual cortex[21–23].

These functional divisions beg the question of how they interact for real world behavior. A prime example is transsaccadic vision: humans make saccades several times per second requiring the visual system to retain, compare and/or integrate information between different visual fixations[24–27]. This is thought to involve a network that includes saccade signals from the frontal and parietal eye fields[5,28], and low-level feature processing in inferior parietal cortex and dorsomedial occipital cortex[29–31]. Further, when saccades reverse the visual field of an object, this requires comparisons of information between the two hemispheres[6,7,32,33], presumably via the corpus callosum[34].

Importantly, nearly everything we know about the modularity of cortical saccade and visual systems is based on 'region-of-interest' analysis: much less is known about the dynamics and topology of these systems at the network level. Recently there has been increased focus on *functional 'connectivity'*, i.e., signal correlations between different cortical regions referred to as nodes[35]. Signal correlation and synchronization, at the level local field potential oscillations or large-scale activity patterns, are thought to be important for local and long-range integration of information across cortex[36–38].

Functional connectivity can be determined for specific 'seed' regions[29,30,39], but more sophisticated techniques like graph theory analysis (GTA) can compute global network properties, including important network 'hubs' and formal measures of functional integration and segregation[40,41]. Most important for our purposes, GTA measures of optimal community structure (groups of highly correlated regions that have few signal correlations with nodes outside of their community) allow one to determine modular organization of cortical regions into functional sub-networks[42–45]. Typically, these techniques have been applied to 'resting state' imaging data[46,47], but we have recently shown that GTA can also be applied to sensory and motor events recorded during active behavior[40].

Here, we performed a GTA / modularity analysis on functional magnetic resonance imaging (fMRI) data collected in a task that involved discriminating changes in the shape versus orientation of a central object with or without an intervening saccade that reversed the visual hemifield of the object (Fig. 1a). A previous region of interest (ROI) analysis of these data confirmed the role of dorsomedial occipital and inferior parietal cortex in transsaccadic feature integration[39]. Here, we derived fMRI time series data across a broad distribution of cortical 'nodes' in the visual system[39,48] and then used GTA to derive formal measures of functional modularity, integration, and segregation between these nodes. With these techniques, we investigated two questions: (1) will lateralization and dorsal-ventral modularity automatically arise from this task and analysis, and (2) will saccades increase functional connectivity in the visual system, specifically across hemispheres.

Results

Figure 1a shows our experimental paradigm. 17 participants fixated either left or right of center and were presented with an oriented object in their periphery. Following a brief mask, an object was once again presented; this object was either the same shape as the first presentation with a new orientation, or a new shape with the same orientation. During *Fixation* trials, gaze remained stable at the original location, but during *Saccade* trials, an eye movement was made to the opposite side, such that the second object appeared in the opposing visual hemifield. The latter condition thus required comparisons between visual information from the same location in space but viewed in opposite hemifields. Experiments were performed within an MRI scanner in complete darkness (*Materials and Methods* for details of experimental methodology). This dataset was previously used for a univariate analysis, which reported widespread contralateral visual field preference (Supplementary Table 1), bilateral saccade modulations in visual cortex, and interactions between the initial and final stimulus when saccades reversed the visual field of the stimuli[39]. It was selected here to provide a rich set of sensory and motor signals for GTA.

To compute GTA measures, we derived group blood oxygenation level-dependent (BOLD) time series from 50 regions of interest (defined here as *nodes*), using coordinates derived from previous studies of the visual system (Fig. 1b; Supplementary Table 1). Superscript symbols[†] in the table indicate overlap with the visual field-specific activation derived from same dataset used here[39].

In the following sections, we first provide global measures of functional integration, then analyze modularity (groups of nodes based on high degrees of correlated activation[44,49], *Eigenvector Centrality* to identify local (within module) hubs, and *Betweenness Centrality* to identify nodes that might be important for propagation throughout the network[43,50]. Note that these measures do not imply causality or anatomic connection but rather provide patterns of signal correlation for system-level function.

Global network features

In graph theory analysis, the *Cluster Coefficient* provides a measure of functional segregation (degree of interconnectivity at a local scale) whereas *Global Efficiency*, is a measure of functional integration (interconnectivity across the entire network); see Methods for details. Both measures showed significant differences between our *fixation* and *saccade* data (Fig. 2). There was a significant increase in *clustering coefficient* during *saccades* ($M = 0.475$, $SD = 0.045$) compared to *fixation* ($M = 0.465$, $SD = 0.039$), $t(16) = -0.02$, $p = 0.036$, and *global efficiency* during *saccades* ($M = 0.481$, $SD = 0.045$) compared to *fixation* ($M = 0.471$, $SD = 0.038$), $t(16) = -0.02$, $p = 0.037$, indicating that eye movements increased functional segregation and functional integration of

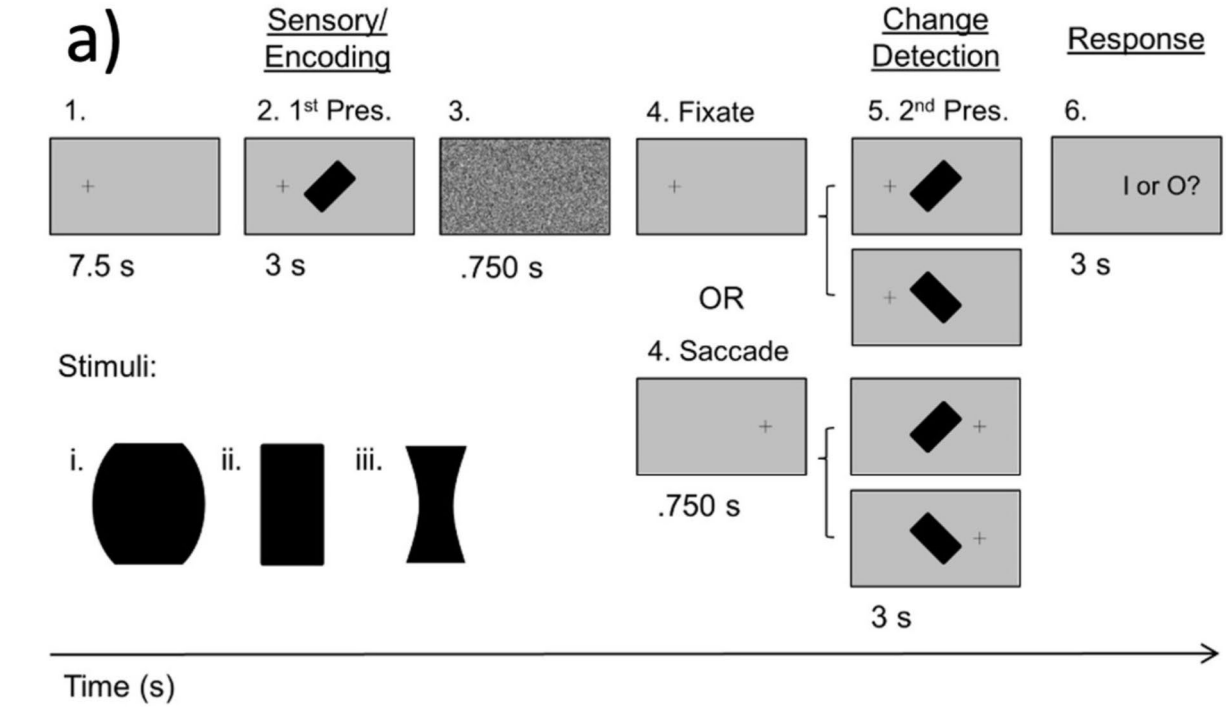

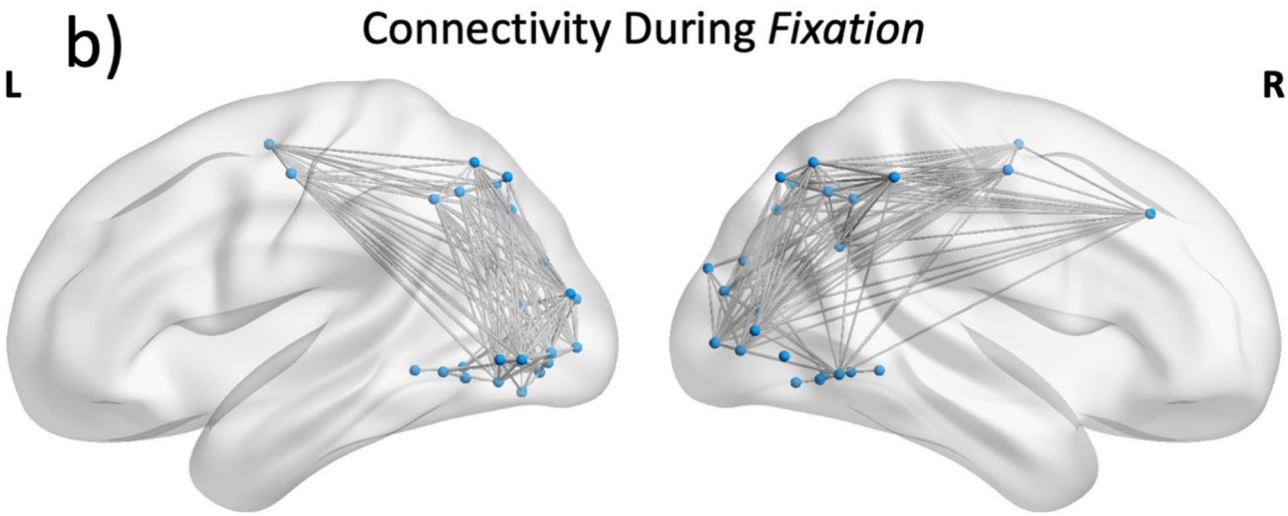

Fig. 1. (**a**) Event-related fMRI experiential paradigm used to identify cortical regions involved in object identity and orientation recognition and the influence of saccades on these processes. (**b**) 50 ROIs that were subjected to the GTA analysis and their correlated activity during *Fixation* trials. These regions are described in Supplementary Table 1. Brain networks were visualized with the Brained Viewer (http://www.nitrc.org/projects/bnv/)[96].

the network respectively. Next, we investigate the organization of these networks at intermediate (modular) and local (eigenvector centrality hub) levels.

Modularity and eigenvector centrality in the fixation task

Our next goal was to determine if functional connectivity in the *Fixation* task shows the kind of modularity suggested by traditional region-of-interest approaches. Figure 3 shows the results of an unsupervised Newman modularity analysis on our 50 nodes[43,49]. The modules are shown as color coded 'nodes' (small dots), 'edges' (lines between the nodes), and hubs (large dots) based on Eigenvector Centrality, a measure of the importance of the node within its module. These hubs were determined by dividing eigenvector centrality values for all nodes in each module by the greatest eigenvector centrality value from that module. Figure 3 labels indicate nodes with normalized eigenvector centrality values above the upper 95th percentile.

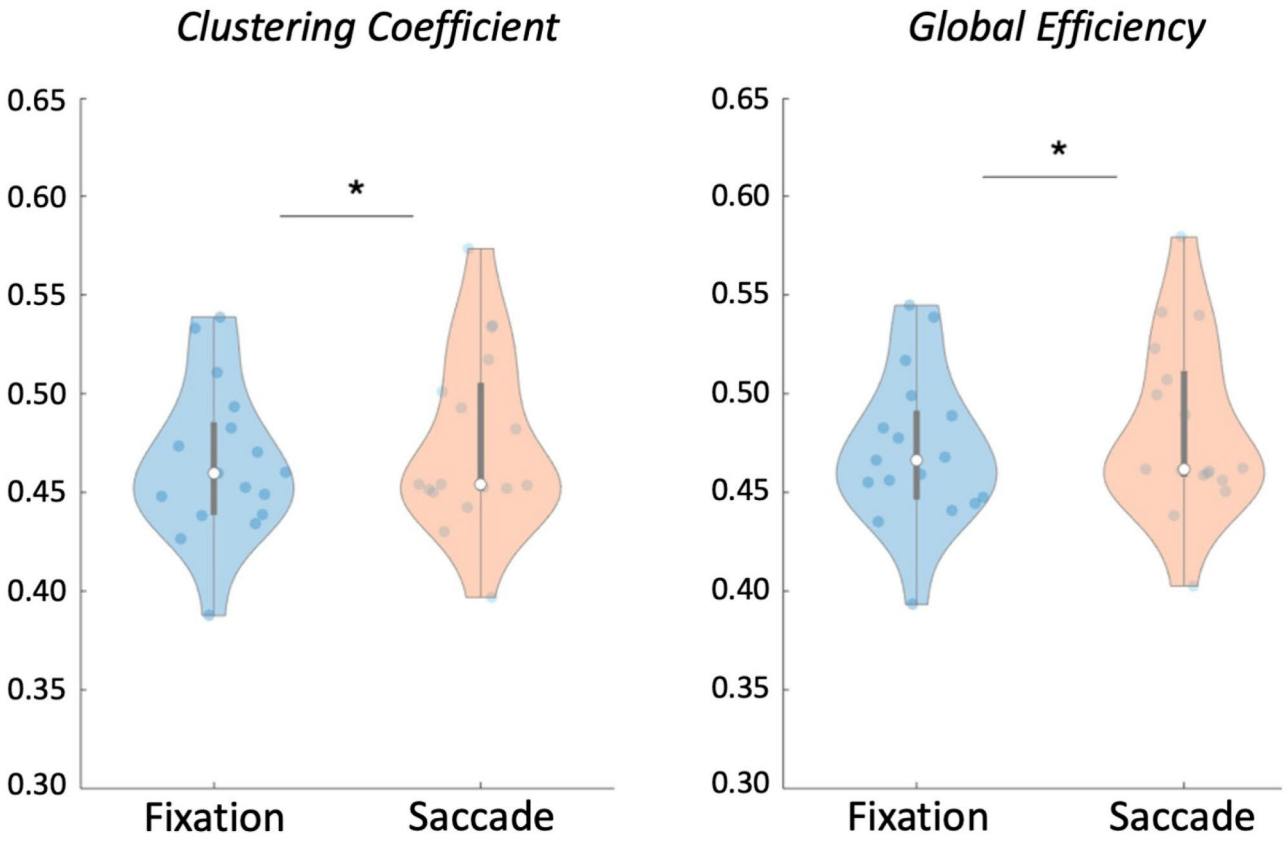

Fig. 2. Results of the functional segregation and functional integration measures. Conditions were compared using nonparametric permutation t-tests ($p < 0.05$). *Left*: Clustering Coefficient, a measure of overall functional segregation in the network, was greater in the *Saccade* condition relative to *Fixation*. *Right*: Global Efficiency, a measure of overall functional integration in the network, was greater in the *Saccade* condition relative to *Fixation*.

Based on the simple assumption that BOLD series correlations would only be driven by the appearance of a stimulus in the contralateral visual field, one might expect our visual system nodes to divide into two unilateral modules in the *Fixation* task: one module in the left hemisphere and one in the right hemisphere. Instead, our nodes were organized into three modules: a bilateral dorsal module that spanned our parietal / frontal nodes in both cortical hemispheres (Fig. 3, green module), a bilateral but asymmetric module that spanned most of our left occipital / temporal nodes and some right nodes (Fig. 3 purple module), and a smaller unilateral module in right occipital / temporal cortex (Fig. 3, orange module). We will next discuss these modules both in terms of their dorsoventral segregation and their lateralization in more detail.

In terms of dorsal-ventral segregation, the dorsal (Fig. 3 green) module appears to correspond to the dorsal attention network[21–23], including nodes associated with such as right dorsolateral prefrontal cortex[51], the frontal eye fields[28,52], and several sites along the intraparietal sulci[53,54]. Eigenvector Centrality Hubs in this module included intraparietal sulcus (IPS1, IPS2, IPS3, and IPS4) and superior parietal lobule (SPL1). In contrast, the ventral (purple and orange) modules included occipital / temporal nodes associated with low-to-high level object feature processing[55], but also some superior occipital nodes associated with the dorsal visual stream[56]. The (mostly) leftward module included Hubs in lateral occipital cortex and visual area V3A whereas the rightward module Hubs included visual areas V3A and V7/ISPO.

The patterns of clustering and segregation observed in our data ultimately arise from similarities and dissimilarities in the BOLD time courses from different nodes. For example, some of our nodes showed a relatively early transient responses, others a more prolonged response, and others a more gradual rising response (Supplementary Figs. 1, 2). A key factor for modularity here was visual field specificity. Most of our visual nodes showed some degree of field specificity (Supplementary Table 1), but the degree of visual specificity varied between different clusters of nodes. BOLD responses from the unilateral 'orange' module nodes were highly field-dependent and thus showed little correlation with responses at the corresponding nodes in the opposite hemisphere (Supplementary Figs. 1A, 2C). Nodes in the dorsal 'green' module showed the least field specificity (Supplementary Fig. 2A), resulting in high correlations across hemispheres. Nodes from the 'purple' module showed an intermediate pattern: a strong contralateral response accompanied by a scaled-down ipsilateral response (Supplementary Fig. 2B), and thus still showed bilateral correlations.

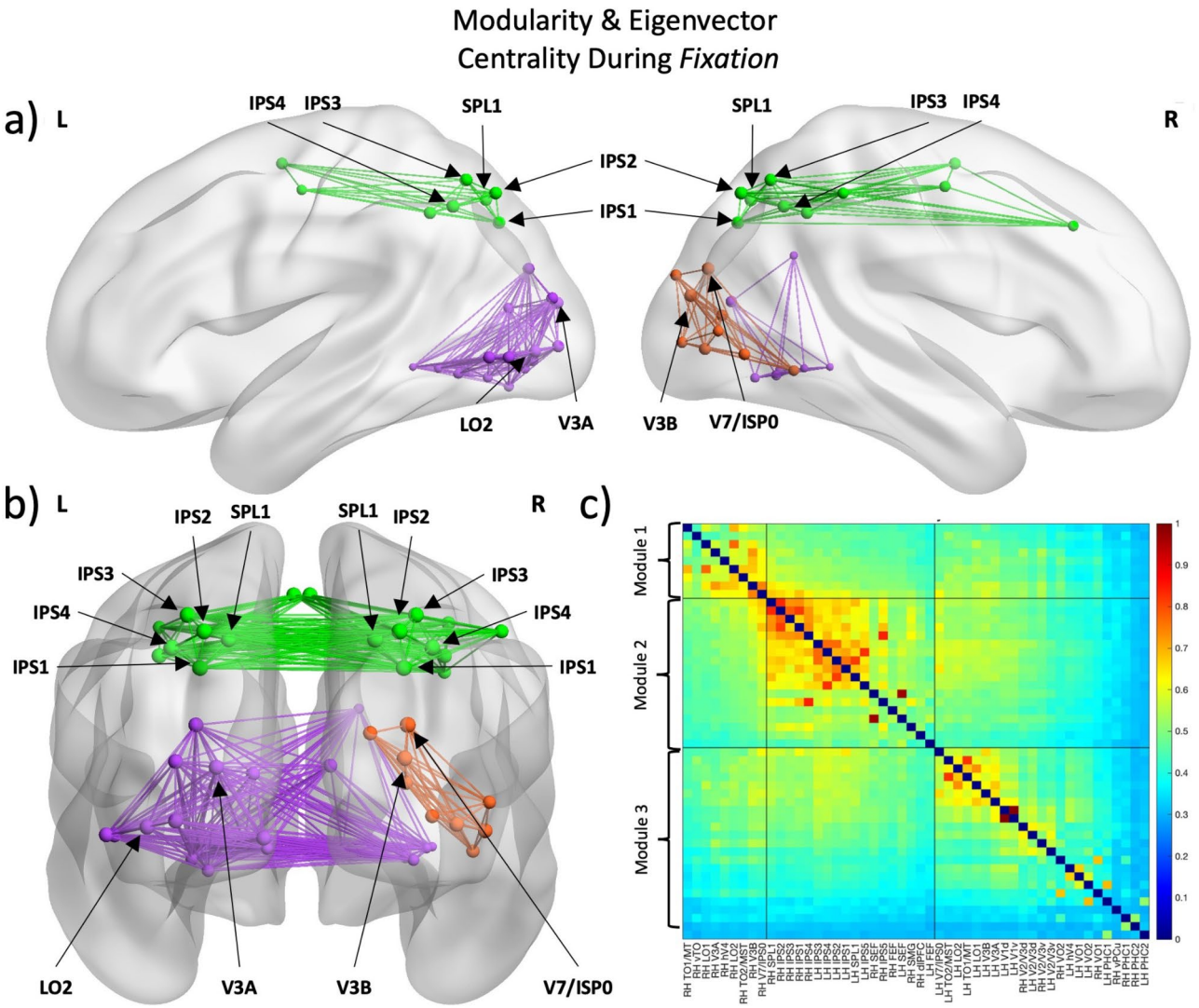

Fig. 3. Modularity results of the *Fixation* condition. (**a**) Lateral views highlight ventral-dorsal modularity in the visual system. Node size demonstrates Eigenvector Centrality with larger nodes being more central within each module (i.e., hub regions). Hubs were computed by normalizing eigenvector values and selecting those with values between 95 and 100. (**b**) Posterior view highlights right-left lateralization modules. (**c**) Adjacency matrices reorganized following modularity analysis. Black lines indicate separation of the ROIs into 3 modules, with the large black squares along the diagonal showing distinct modular groups. Brain networks were visualized with the BrainNet Viewer (http://www.nitrc.org/projects/bnv/)[96].

Influence of saccades on modularity and eigenvector centrality

Our next goal was to determine the influence of saccades on the modular networks described in the previous section. Recall that in our paradigm, saccades reversed the visual hemifield (and thus the cortical hemisphere) used to view the second visual stimulus relative to the first stimulus, and then participants compared the stimuli. We hypothesized that the combination of bilateral saccade signals[39], 'remapping' signals across hemispheres[30,32,39] and the physical sensory stimulus would increase bilateral functional connectivity.

Figure 4 shows the results of a Newman modularity analysis of the fMRI data from our *saccade* condition. Overall, dorsal-ventral modularity was preserved during *saccades* (Fig. 4), except two regions (bilateral V7/IPS0) switched from the dorsal fixation module to the ventral modules during *saccades*. More importantly, during *saccades* the two ventral modules combined into a single bilateral module. This is most clear from the posterior view of the brain (Fig. 4b). The reason for these results can again be seen in the underlying BOLD responses (Supplementary Figs. 1, 2). The post-saccadic response is delayed because of the temporal separation of cues in our event-related fMRI paradigm but still results in a correlation of signals across hemispheres. Nodes in the 'orange' *fixation* module now show a response whether the pre-saccadic or post-saccadic stimulus appears the contralateral field (Supplementary Fig. 1B). Signals that were already correlated in the 'green' and 'purple' *fixation* modules (Fig. 3) and across visual fields (Supplementary Fig. 2) simply continued to correlate during *saccades*.

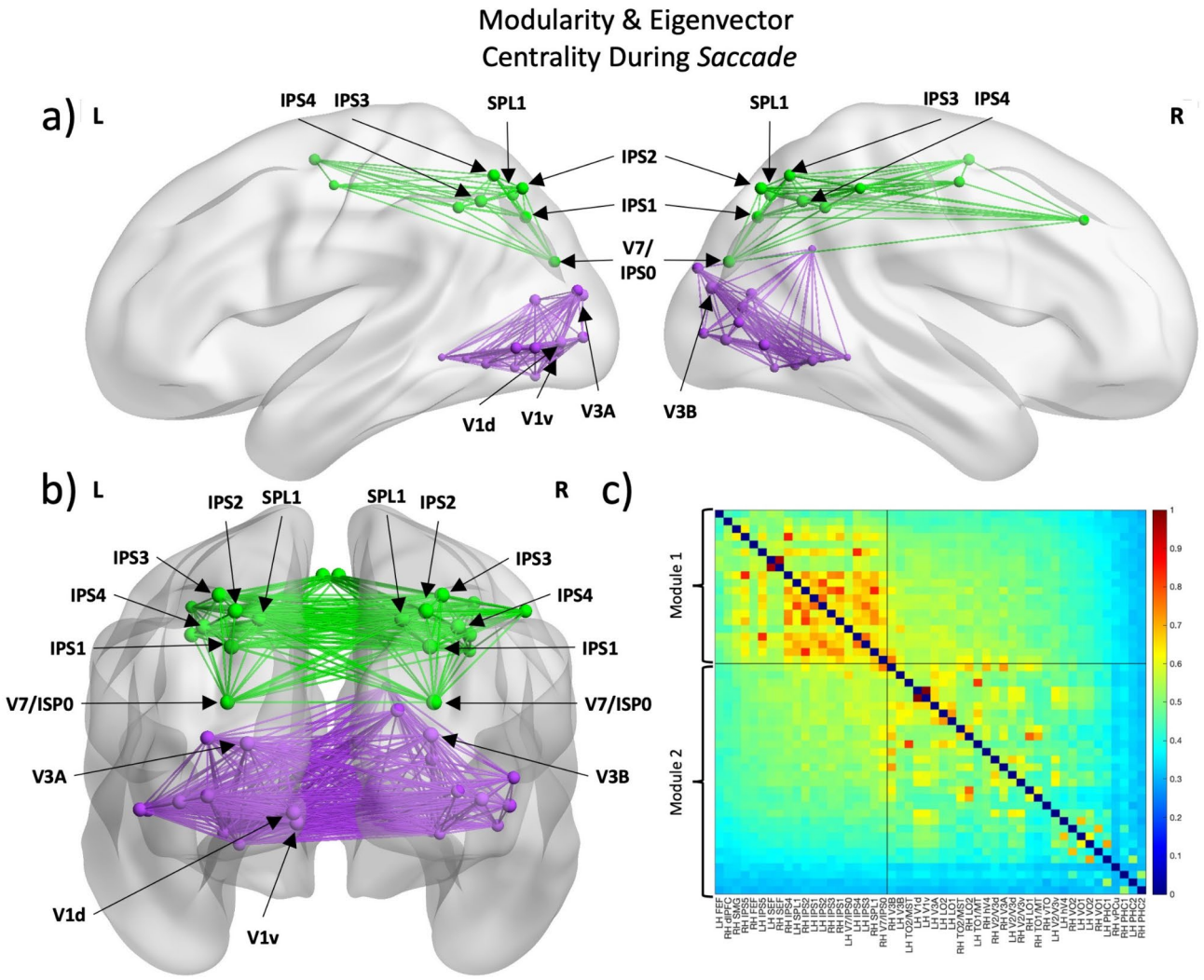

Fig. 4. Modularity results of the *Saccade* condition. (**a**) Lateral views highlight dorsal-ventral modularity in the visual system. Node size demonstrates Eigenvector Centrality with larger nodes being more central within each module (i.e., hub regions). Hubs were computed by normalizing eigenvector values and selecting those with values between 95 and 100. (**b**) Posterior view shows that the two right-left lateralized modules become highly intercorrelated, resulting in a single module. (**c**) Adjacency matrices reorganized after modularity analysis. Black lines indicate separation of the ROIs into 2 modules, with the large black squares along the diagonal showing distinct modular groups. Brain networks were visualized with the BrainNet Viewer (http://www.nitrc.org/projects/bnv/)[96].

To quantify the extent to which modularity was altered during *saccades*, we conducted a quantitative analysis on the sets of nodes that were identified to be part of the dorsal and ventral pathways during both conditions (excluding bilateral V7/IPS0, since these were the only nodes that changed their activity between both pathways). There was no significant change in the degree of modularity for the nodes in the dorsal pathway. However, in the ventral nodes showed increased modularity during *saccades* (M = 0.951, SD = 0.05) compared to *fixation* (M = 0.941, SD = 0.04), t(16) = -0.017, $p = 0.002$, (nonparametric t-test) in the ventral pathway, indicating significantly increased functional connectivity and temporal signal sharing between these regions (Fig. 5).

At first glance, Eigenvector Hubs in the *Fixation* (Fig. 3) and *saccade* (Fig. 4) modules appear to be very similar. To quantify this more rigorously, we performed a direct statistical comparison between Hubs in the *Fixation* and *Saccade* conditions (Fig. 6, see caption for detailed statistics). We found that the *saccade* condition showed significantly higher Eigenvector Centrality in four of our occipital nodes, including 3 in the left hemisphere (V1v, V2/V3v, V1d, and V2/V3d) and one in the right hemisphere – V2/V3v. These are areas that have been previously implicated in transsaccadic integration of feature and shape information[29,39].

Communication between modules: betweenness centrality

The application of Eigenvector Centrality to cortical nodes in Figs. 2 and 3 informs one about the importance of certain hubs *within* modules. Assuming these modules are not completely independent, it was also of interest to

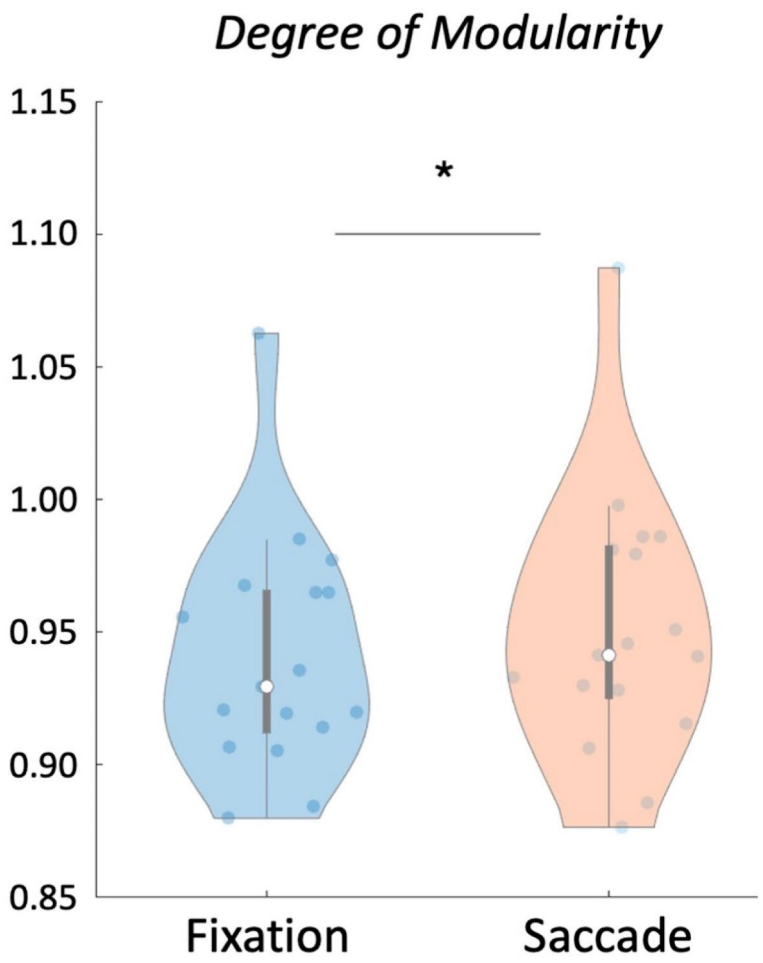

Fig. 5. Results of the degree of network modularity comparison for the ventral nodes. Conditions were compared using nonparametric permutation t-test ($p < 0.05$). Higher values here indicate greater functional connectivity in the ventral nodes in the *Saccade* condition relative to *Fixation*.

determine which nodes of each module act as important hub regions that 'bridge' *between* modules. Betweenness Centrality is a measure that determines which nodes facilitate functional integration between modules[43,50].

Figure 7 denotes the nodes with greatest Betweenness Centrality of each module in the *Fixation* and *Saccade* conditions, respectively. The plotting conventions are like Figs. 3b and 4b, except prominent 'between module' edges have now been added (grey lines). During *fixation* (Fig. 7a), bilateral intraparietal sulcus areas IPS3 and IPS4 were identified as important Betweenness hubs for the bilateral dorsal (green) module, whereas bilateral V3B played this role in the two ventral networks. During *saccades* (Fig. 7b), only bilateral intraparietal sulcus (IPS4) and right dorsomedial occipital cortex (V3B) were preserved as important hubs for communication between the two remaining dorsal and ventral modules. In this case, no significant differences were found between *fixation* and *saccade* hubs, but both the posterior parietal and dorsomedial occipital cortex hubs have been previously implicated in transsaccadic feature integration[5,30,31,39].

Discussion

In this study, we analyzed the network organization of the visual system during an active visual behaviour. Specifically, we subjected correlated BOLD activation of 50 ROIs to a set of GTA measures and contrasted these between our *Fixation* and *Saccade* conditions. Overall, *saccades* increased interconnectivity of the network at both global and local levels. Our analysis of modularity in the *Fixation* condition revealed three sub-networks: a single bilateral dorsal group, and two lateralized ventral groups with three important hubs for information propagation throughout the network: bilateral IPS3, IPS4, and V3B. In the *Saccade* condition, the two ventral sub-networks were combined into a single ventral sub-network, consistent increased connectivity between the hemispheres for processing information across the two hemifields. We found that the degree of modularity of the ventral nodes increased during *saccades*. Additionally, V1v, V1d, V2/V3v, and V2/V3d in the left hemisphere, and V2/V3v in the right hemisphere emerged as important ventral hubs in the *saccade* condition.

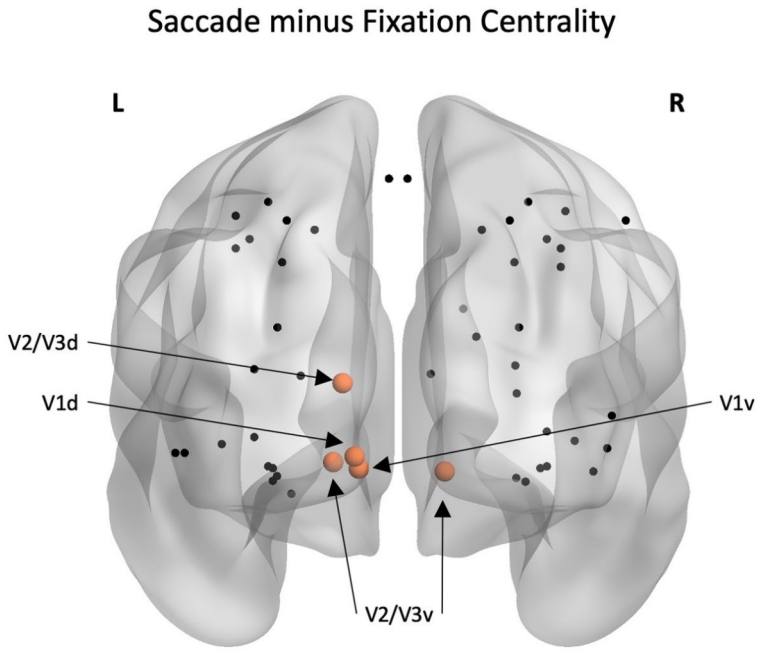

Fig. 6. Node Eigenvector Centrality compared across the *Fixation* and *Saccade* conditions. The four regions in orange were significantly more central during *Saccade* relative to *Fixation*. Conditions were compared using nonparametric permutation t-tests and false detection rate (FDR) was used to control for multiple comparisons. Adjusted *p*-values ($p_{adj} < 0.05$) are reported here. These regions include 4 regions of the left hemisphere – V1v [*saccade* (M = 0.152, SD = 0.008); *fixation* (M = 0.148, SD = 0.009); t(16) = − 0.007, p_{adj} = 0.008], V2/V3v [*saccade* (M = 0.137, SD = 0.008); *fixation* (M = 0.129, SD = 0.007); t(16) = − 0.010, p_{adj} = 0.002], V1d [*saccade* (M = 0.153, SD = 0.009); *fixation* (M = 0.149, SD = 0.008); t(16) = − 0.007, p_{adj} = 0.008], and V2/V3d [*saccade* (M = 0.143, SD = 0.006); *fixation* (M = 0.138, SD = 0.008); t(16) = − 0.009, p_{adj} = 0.004] – and a single region of the right hemisphere – V2/V3v [*saccade* (M = 0.142, SD = 0.007); *fixation* (M = 0.135, SD = 0.008); t(16) = − 0.010, p_{adj} = 0.002]. Brain networks were visualized with the BrainNet Viewer (http://www.nitrc.org/projects/bnv/)[96].

Caveats and limitations

Before considering these results further, we acknowledge several caveats and limitations. First, the choice and definition of nodes[57–59]. Our selection of 50 nodes was guided by our focus on the visual system, i.e., published, interpretable visual regions, and thus does not represent a 'whole brain' analysis[60,61]. Second, this approach necessitated the use of fixed node coordinates, which might obscure intersubject differences[58,62,63]. Third, although we intentionally chose a dataset that incorporates saccades and several object features, our results may not translate to other visual tasks. Fourth, it is possible that adjacent nodes shared overlapping visual signals, exaggerating local correlations. Finally, GTA relies on signal correlations, and thus cannot prove either anatomic connections or causality. Given these caveats, we will interpret our results with respect to the physiology and anatomy of the system.

Global network features

To analyze the overall local and global properties of the network, *clustering coefficient* and *global efficiency* were used respectively. Clustering coefficient is a measure of functional segregation that provides a value for the degree of interconnectivity at a local scale by investigating closed circuits in the network, with higher values indicating powerful processing at localized levels. Global Efficiency, in contrast, is a measure of functional integration that provides a value for the degree of interconnectivity at a global scale by investigating the shortest paths information travels throughout the network, with higher values indicating efficient information propagation between distant nodes. Here, saccadic eye movements led to significant increases in both functional segregation and integration (Fig. 2), indicating that saccades shaped in the network at both local and global levels to maximize efficiency of processing. It is noteworthy that these results are identical to the findings of Ghaderi et al.[40], despite their use of EEG (as opposed to fMRI) to contrast *saccade* versus *fixation*. These findings are consistent with the idea that transsaccadic integration requires the visual system to integrate multiple information streams[4] and again, to share information across visual fields[6,7].

Dorsal-ventral modularity during fixation

The dorsoventral modularity observed here is reminiscent of the two-streams hypothesis of vision, based in the neurophysiology, neuropsychology, and neuroimaging literature[3,4,10–12]. This hypothesis has been critiqued for various reasons[64–66] but continues to shape our understanding of the visual system. Despite similarities to this classic view our results also differed in ways considered below.

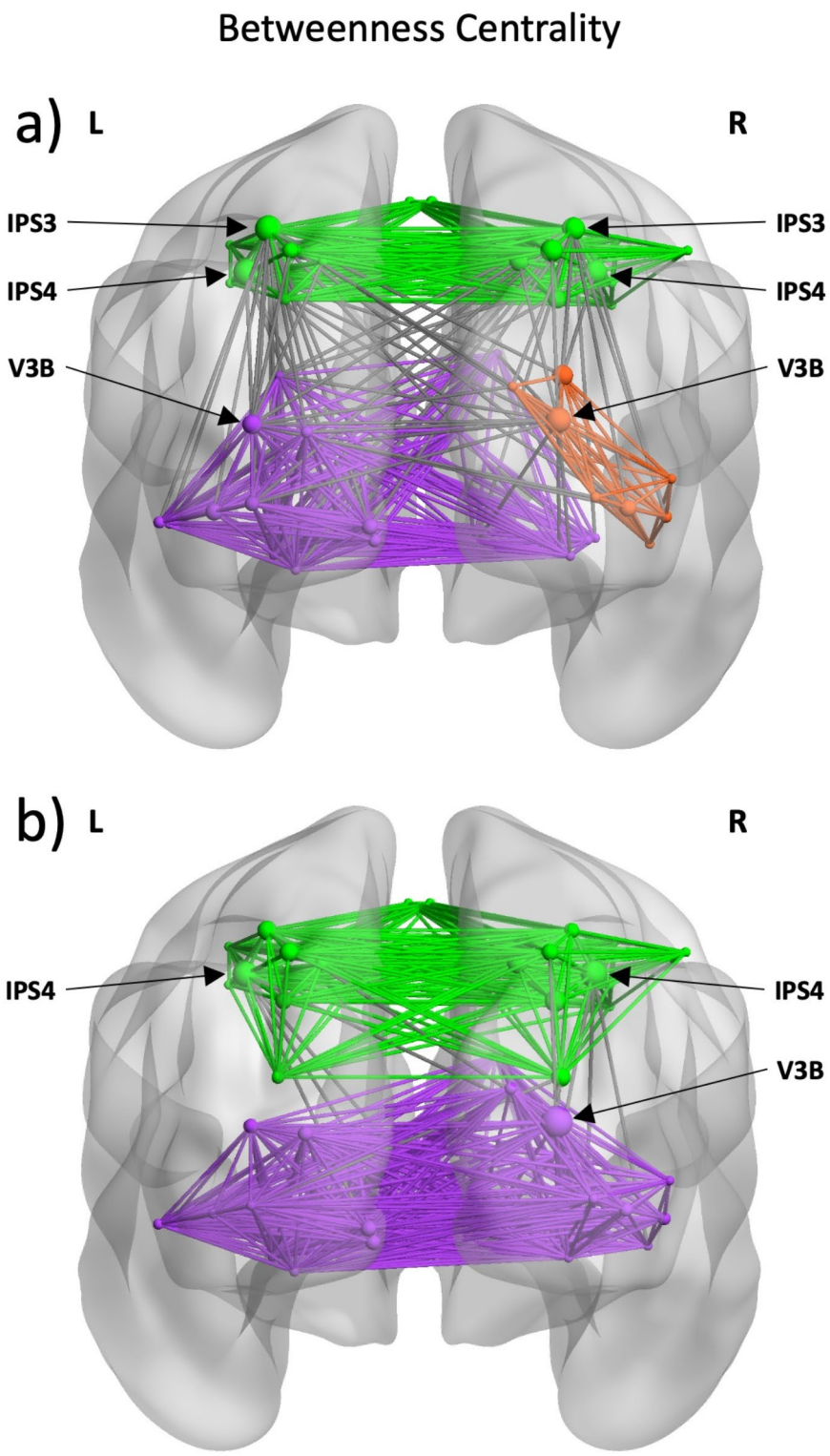

Fig. 7. Betweenness Centrality hubs are labeled by normalizing betweenness values and selecting those with normalized values between 85 and 100. The conventions are similar to Figs. 3b and 4b, but 'between module' edges have been added (grey lines). (**a**) Modularity and Betweenness Centrality results of the *Fixation* condition. None of the nodes in the purple module satisfied the normalized betweenness value criteria; left V3B is labeled as the node with the highest Betweenness Centrality in the purple module. (**b**) Modularity and Betweenness Centrality results of the *Saccade* condition. Brain networks were visualized with the BrainNet Viewer (http://www.nitrc.org/projects/bnv/)[96].

An advantage of the GTA approach is that it does not rely on (potentially) biased interpretations, but rather on an objective, unsupervised network analysis. Essentially, our modularity analysis grouped or segregated nodes based on similarity or dissimilarity of their BOLD time series (Supplementary Figs. 1, 2). This analysis revealed a dorsal module that spanned nodes and 'within module hubs' ranging from parietal areas like V7 and intraparietal cortex to prefrontal areas including the frontal eye fields and dorsolateral prefrontal cortex whereas our ventral modules spanned traditional visual areas (V1, V3, parahippocampal cortex) in occipital-temporal cortex.

While this generally supports a two-stream hypothesis, it differs from the traditional view of perception-action segregation *within* occipital cortex[3,4,10–12]. This might be because early dorsoventral modularity requires the presence of an overt action, such as a reach movement[67], which did not occur in the current experiment. Instead, the dorsal-ventral modularity in our task / network may have been driven by the distinction between attention for saccade targets versus visual features[68–70]. This notion aligns with the two-stream attention system theory[71], involving a dorsal network for spatial attention, saccade planning / execution, and visual working memory[72–74] versus a ventral attention system associated with feature processing and (when damaged) hemispatial neglect[71,75–77].

Lateralization during fixation

Interestingly, our dorsal parietofrontal network was bilateral, whereas our ventral modules were highly lateralized, with the larger ventral module mostly spanning left cortex, and the other smaller module localized to the right hemisphere. This result does not conform to the expectation of a simple lateralized system based on strict opposite-field specificity. Instead, this result seems to be shaped by different degrees of visual field specificity (Supplementary Figs. 1, 2), suggesting different degrees of bilateral communication in the visual system, at least at the level of the BOLD signal / synaptic input[78]. This in turn suggests that the dorsal module is specialized for spatial computations that inherently require global (cross field) visual processing whereas the ventral networks might be more concerned with local feature processing.

This conclusion is consistent with the notion of a bilateral dorsal attention system that includes IPS and FEF as important regions, and a lateralized ventral attention system[23,71,74,79,80]. Further, the asymmetric lateralization in our ventral modules is consistent with the asymmetry observed in hemispatial neglect, i.e., where right damage produces profound localized deficits in the left visual field whereas left damage produces more subtle deficits[76,77]. Specifically, right hemispheric damage would obliterate our right ventral module, whereas the rightward nodes of the more distributed 'left' module would survive left hemisphere damage.

Influence of saccades

Our hypothesis was that saccades would increase signal sharing between the two hemispheres, due to the need for integrating visual information from opposing hemifields in the task, a phenomenon referred to as transsaccadic integration [24, 28}. We did not observe any major changes in the dorsal network, presumably since it was already bilateral connected. The most dramatic effect of saccades that was the 'joining' of the two ventral modules due to increased correlation (Fig. 4, Supplementary Fig. 1B). Again, this does not appear to be specific to fMRI, because we observed a similar effect during EEG recordings[81]. Three factors could contribute to effect: saccade motor signals, remapping signals, and the appearance the pre- and post-saccadic stimuli on opposite visual fields.

It might be assumed that saccade signals are constrained to the saccade motor system, but they are observed in BOLD signals throughout the visual system[29,30], at least implying synaptic activity[78]. In our previous univariate analysis (of the same dataset used here), we observed bilateral saccade activation across occipital areas corresponding to our ventral modules here[39]. These bilateral modulations could contribute to the increased correlations between these modules observed here during the saccade task.

Second, transsaccadic feature integration is thought to build on the neural mechanisms for *spatial updating*[24,28], the attention-dependent process that accounts for changes between the observer and the environment during self-motion[70,80,82]. This in turn is thought to result in remapping of visual signals, which may provide the subjective sense of space constancy during saccades[83]. Previous studies have shown that updating / remapping can occur between the two hemispheres when saccades reverse visual hemifields[6,7,32], presumably via the corpus callosum[36]. Since we previously observed interactions between pre-saccadic and post-saccadic stimulus response in this same dataset[39] it is likely that remapping signals contributed to the bilateral correlations in the current dataset.

Finally, the physical appearance of the post-saccadic stimulus in the opposite hemifield clearly produced activation that contributed to the bilateral correlation. It is noteworthy that the post-saccadic response (perhaps a combination of saccade, remapping, and sensory inputs) was delayed by design from the presaccadic response in our paradigm (Supplementary Fig. 1) but in real world conditions this delay would only be about (50-100ms). In this real-world situation, anticipatory remapping signals would increase bilateral communication even before the saccade begins[24,84]. Regardless of the underlying mechanism, the important result here is that the correlation between pre- and post-saccadic activity is likely an important mechanism for the brain's ability to integrate or compare information across saccades.

Saccade-related network hubs

Our *fixation* modules already included hubs that have been implicated in saccades and transsaccadic integration, including the right dorsolateral prefrontal cortex[85], the frontal eye fields[28,40,52] the lateral and medial intraparietal sulci[29–31], and dorsomedial occipital cortex (V3B)[30,39]. Most of these hubs persisted during saccades, so to evaluate their specific roles, we contrasted eigenvector centrality between the two conditions.

This contrast identified five major local hubs in the occipital lobe following FDR correction, further highlighting the increased interconnectivity of the ventral nodes, four regions in the left hemisphere (V1v, V2/V3v, V1d, and V2/V3d) and one in the right hemisphere (V2/V3v). This suggests that these areas are more central and interconnected within the ventral modules during saccades. The regions that emerge here are all visual cortex regions that are involved in early processing of visual information for transmission to higher-order processing areas[10]. Since this information becomes widely distributed along both dorsal and ventral pathways following early processing in V1, it is reasonable that these early focal points are highly locally connected with those subsequent regions and thus high in Eigenvector Centrality. These visual cortex areas are also heavily involved in remapping during transsaccadic integration, communicating with an intricate network of regions[7,32,39]. We did not find any significant difference in Betweenness Centrality for *Saccades* relative to *Fixation*, but within the *saccade* dataset we observed that bilateral IPS3 and left V3B's were important for long-range information propagation across the network.

Communication between modules

Our results do not suggest a complete dissociation between modules. Specifically, our analysis of global network properties shows that the entire network of 50 ROIs is both functionally segregated and integrated with heightened interconnectivity at both local and global levels (Fig. 2). This suggests that, despite modular specialization within the system, the overall network remains interconnected to facilitate rapid and effective global transmission of information. This is expected from a network that must integrate perception and action for real-world behavior[28,65].

More specifically, our betweenness centrality analysis identified bilateral regions of both the dorsal and ventral pathways as significant 'bridge' nodes for intermodular communication. These include the intraparietal sulcus (IPS) in the dorsal module and area V3B in the ventral modules (Fig. 7). The IPS is considered a significant region of the dorsal attention network that is involved in spatial attention, eye movements, reaching and grasping[17,29,74,75]. Conversely, area V3B is known for its retinotopic representation of foveal and peripheral vision[86] and for connecting early visual areas in the occipital lobe with higher order visual processing in the parietal lobe[87]. These regions thus emerge as significant hubs for cross-network communication of spatial attention and working memory[88], and communication between different levels of visual processing.

Conclusions

In conclusion, we employed graph theory analysis to evaluate the modularity and saccade-dependence of fMRI BOLD signals derived from 50 visual regions, acquired from participants engaged in a shape / orientation change discrimination task, with or without intervening saccades. Our primary results were that (1) during *Fixation*, three sub-networks of the cortical visual system emerged: a single bilateral dorsal module spanning nodes in parietal-frontal cortex, and two lateralized ventral modules spanning nodes in occipital-temporal cortex, (2) during *Saccades*, the two ventral sub-networks amalgamated into a single, bilateral module, and (3) saccades also increased the overall interconnectivity of the network at both global and local levels. These results provide objective confirmation of signal modularity in the visual system and show that saccades have a profound influence on the network properties in this system. Specifically, resulting in global and cross-module correlations that could contribute to the brain's ability to integrate information across gaze fixations, for continuous visual perception.

Materials and methods

Participants

On the basis of a power analysis performed with an effect size (0.887) obtained from the most relevant region (right SMG) in a recent transsaccadic study[29], we determined that 13 participants would be sufficient to achieve an overall power of 0.914[39]. This analysis was performed using G*Power[89] with the following parameters: (1) two-tailed repeated measures t-tests, (2) a desired power value of 0.90, and (3) an alpha value of 0.05. 21 right-handed participants with normal / corrected-to-normal vision and no history of neurological disorders were tested. Of these, 17 participants (mean age: 28.7 +/- 5.2, 12 females) passed our inclusion criteria for further analysis[39]. All participants provided written informed consent and were compensated for their time. This experiment was approved by the York University Human Participants Review Committee (HPRC). All experiments were performed in accordance with HPRC guidelines and the Declaration of Helsinki.

Experimental set-up and stimuli

Participants were required to pass MRI screening and were asked to assume a supine position on the MRI table. Their head lay in a 64-channel head coil. A mount on the head coil was used to support an infrared eye-tracker (for the right eye) to ensure appropriate fixation/eye movements, as well as a mirror that reflected the image of the screen from inside the MRI bore. Participants held a button box with their right hand (index and middle fingers rested on the first and second buttons, respectively). Button press responses were analyzed offline.

The experiment (Fig. 1) was conducted in complete darkness. A fixation cross was used and always present (except during the presentation of the mask) to direct participants' gaze as required by the task. The fixation cross could appear approximately 7° from either the left or right edge of the gray screen (45.1° x 25.1°) along the horizontal meridian. The black stimulus always appeared in the center of the screen and was either a: (1) rectangle, (2) barrel, or (3) hourglass. The dimensions of the rectangle were 12° x 6°; the other two objects had the same area as the rectangle.

General procedure

Experiment

As show in in Fig. 1, an event-related fMRI design was used whereby each trial commenced with a fixation of a cross, presented either to the left or right center, for 7.5 s. Then, the central object (rectangle, barrel-shaped, or hourglass-shaped object) appeared for 3 s at +/− 45° from vertical. This was followed by a static noise mask for 0.75 s to avoid an afterimage. The fixation cross would then appear either at the same position as before the mask (*Fixation* condition) or at the other location (*Saccade* condition) for 0.75 s. The same object presented at the other possible orientation (Orientation change condition) or one of the remaining two objects presented in the same orientation (Shape change condition) appeared in center for 3 s. The object disappeared and the fixation cross was replaced by an instruction ('I or O?') for 3 s, directing participants to indicate if the two objects presented in the trial changed in shape (first button, 'I') or in orientation (second button, 'O'). Thus, there were four main conditions: (1) *Fixation*, Orientation change, (2) *Fixation*, Shape change, (3) *Saccade*, Orientation change, or (4) Saccade, Shape change. These trial types were randomly intermingled within a run (24 trials); there were eight runs in total. Each run began and ended with central fixation for 18 s to establish baseline measures.

Imaging parameters

We used a 3T Siemens Magnetom Prisma Fit magnetic resonance imaging (MRI) scanner. Functional experimental data were acquired with an echo-planar imaging (EPI) sequence (repetition time [TR] = 1500 ms; echo time [TE] = 30 ms; flip angle [FA] = 78°; field of view [FOV] = 220 mm × 220 mm, matrix size = 110 × 110 with an in-slice resolution of 2 mm × 2 mm; slice thickness = 2 mm, no gap) for each of the eight runs in an ascending, interleaved manner. A total of 312 volumes of functional data (72 slices) was acquired. In addition to the functional scans, a T1-weighted anatomical reference volume was obtained using an MPRAGE sequence (TR = 2300 ms, TE = 2.26 ms; FA = 8°; FOV = 256 mm x 256 mm; matrix size = 256 × 256; voxel size = 1 × 1 × 1 mm^3). 192 slices were acquired per volume of anatomical data.

Analysis

Behavioural data

Eye movements and button presses were recorded throughout the experiment, both of which were analyzed offline for correct fixation and production of saccades. Trials where participants made eye movements when not required to were excluded from further analysis. Similarly, trials where incorrect button presses were made were not included in additional analyses. As a result, for 17 participants, 148 trials were removed (out of 3264 trials; 4.5%).

Functional imaging data

Functional data from each run for each participant were preprocessed (slice time correction: cubic spline, temporal filtering: <2 cycles/run, and 3D motion correction: trilinear/sinc). A Talairach template[90] was used to transform raw anatomical data. Functional data were co-registered via gradient-based affine alignment (translation, rotation, scale affine transformation). A last step of preprocessing involved applying smoothing using a FWHM of 8 mm.

General linear models (GLMs) were created (BrainVoyager QX 20.6; Brain Innovation) for each run across all participants. Each GLM included four predictors, one for each of the four main conditions: (1) "FixOC", for *fixation* trials during which only the orientation of the same object changed; (2) "FixSC", for fixation trials during which only the shape of the object changed; (3) "SaccOC" for saccade trials where only the orientation of the object changed; and (4) "SaccSC" for *saccade* trials where only the shape of the object changed. Each of the four predictors were convolved with a hemodynamic response function (standard two-gamma function model)[35]. Final modifications of GLMs were made to include an "Error" confound predictor for trials during which participants made eye movement and/or button press errors.

FMRI signal extraction

To carry out the analyses, spheres were created around a central Talairach coordinate for each a priori-defined region-of-interest (ROI; see Supplementary Table 1). The ROIs were created using BrainVoyager QX v2.8 with a radius of 3 mm. Raw intensity signals were extracted (BrainVoyager QX v2.8; Brain Innovation) from each of these spheres for each run across all participants which were used to carry out functional connectivity analysis.

Regions of interest

The 50 regions included in our GTA analysis, their abbreviations, and their Talairach coordinates are summarized in Supplementary Table 1. Superscripts[†] indicate nodes that showed visual field specificity in our previous study[39]. ROIs were selected based on previously identified regions involved in visual processing and saccades. Specifically, we used all of the coordinates provided in a probabilistic atlas of standardized visual regions[48]. We supplemented this with several ROIs described in our previous transsaccadic integration fMRI studies[29,30,39]. Some of these ROI coordinates were unilateral, but removing these asymmetries had little or no effect on modularity (Supplementary Fig. 3).

Graph theory analysis

To construct the functional networks and compute network properties, we calculated correlations of BOLD activation across our 50 ROIs. Data from the entire trial (Fig. 1A) were used, which included visual stimuli for approximate 1/3 of the time. Initially, these correlations were conducted for each run and then averaged across runs per *Fixation* and *Saccade* condition for each participant. We then normalized each averaged adjacency matrix by dividing each value by the strongest correlation per participant in each of the two conditions in

accordance with best practice guidelines[45]. For each participant, the resulting values were placed in 50 × 50 adjacency matrices whereby each row (and column) represents a ROI, and their intersection in the matrix communicated the normalized correlation value with each array indicating the functional connectivity between regions; GTA measures were then conducted on these matrices for each participant using the Brain Connectivity Toolbox for MATLAB[41]. Supplementary Fig. 4 shows the weighed, undirected, adjacency matrices of averaged, normalized correlations across participants for each of the *Fixation* and *Saccade* conditions; these averaged matrices were used in the modularity analysis. In this section we present a brief description for GTA.

Modularity, a measure of optimal community structure, attempts to partition nodes in a network into modules consisting of highly interconnected nodes that have few connections with nodes outside of their modular community[43,44]. In the brain, such modules are considered specialized sub-networks of regions organized in such a manner that facilitates information processing among modular regions. Here, we conducted a modularity analysis using the *modularity* function for undirected matrices of the Brain Connectivity Toolbox for MATLAB[41] and a standard γ value of 1.0.

To evaluate modularity of subnetworks, we implemented a Newman modularity algorithm[49] in MATLAB 2019b (open access code for this analysis is available at https://github.com/AHGhaderi/Amir-Hossein-Ghaderi/commit/df636b2105e578a8969ffa88856e54f3267a40a7). The steps to compute modularity are as follows: first, a group of nodes is selected as a subnetwork. For the purposes here, we isolated the nodes from either the dorsal or ventral modules that resulted from the modularity analysis (Figs. 3 and 4), and the average connectivity between these selected nodes was calculated. Next, the connections (i.e., 'edges') between all nodes in the original network were randomly shuffled and then the average connectivity of our selected dorsal and ventral subnetworks was calculated. With these 2 subnetwork averaged connectivity values calculated, we divided the vales of the original subnetworks and the randomized subnetworks. Significant differences between our subnetworks and randomized subnetwork edges demonstrate that the original subnetworks were modular to a high degree.

Clustering coefficient measures functional segregation by quantifying the extent to which a given node's neighbours also neighbour each other[43,91], generating closed 'triangle' circuits in the network. The mean clustering coefficient for the entire network represents the prevalence of clustering around nodes in the network and high clustering coefficients imply high degrees of functional segregation[41]. In brain networks, these segregated 'triangle' circuits account for powerful processing at the local level. Here, we measured clustering coefficient using the adjacency matrices for each condition (*Fixation* and *Saccade*) per participant. Differences in mean clustering coefficient across conditions demonstrate greater interconnectivity between nodes on a local level (i.e., functional segregation) in the condition with greater functional segregation.

Global efficiency measures the average inverse shortest path length - the minimal path of nodes and edges that connect two nodes in a network[42] to determine the connectivity between disconnected or distant nodes within a network[41,91,92]. In biological networks, average global efficiency is the network's ability to transfer information between regions or circuits that are anatomically disconnected but whose communication is necessary to carry out a task. Higher global efficiency is indicative of functional integration of such distant regions (nodes) or circuits of regions (modules). By calculating the difference between global efficiency in our conditions, we can determine changes in functional integration during saccades.

Segregating a network into modules with few connections between sub-networks implies the existence of important 'bridge' nodes that serve as connections. We identified these by calculating Betweenness Centrality, which calculates the number of shortest paths – paths that connect any 2 nodes with the least number of edges – that cross each node. Nodes with high Betweenness Centrality are considered important for the overall communication of a graph because of the high degree of traffic that passes through them. In the brain, these are important hub regions that relay information and facilitate functional integration between different areas of the brain[43,50]. Likewise, Eigenvector Centrality is indicative of a node's centrality within a module or cluster of nodes. The degree to which a node is central for the network can vary across different conditions, indicating that different regions are differentially involved in task-dependent information transfer.

Statistical analyses

Nonparametric permutation t-tests with 25,000 random iterations were conducted to compare graph theory indices between the *Fixation* and *Saccade* conditions. Nonparametric permutation tests are robust to multiple comparisons and produces results similar to general linear models with multiple comparison corrections[93]. For comparison of functional segregation and functional integration, clustering coefficient and global efficiency measures were used respectively. Additionally, Betweenness Centrality and Eigenvector Centrality measures were compared across conditions for each of the 50 ROIs (Supplementary Table 1) to identify significant hub region changes. To control for these multiple comparisons, false detection rate (FDR) was applied for error correction and an adjusted p-value (p_{adj}) of 0.05 using FDR was adopted for significance[94,95].

Data availability

The datasets used and/or analyzed during the current study are available from the corresponding author on reasonable request.

Received: 24 May 2024; Accepted: 21 March 2025
Published online: 28 March 2025

References

1. Sperry, R. W. Cerebral organization and behavior: the split brain behaves in many respects like two separate brains, providing new research possibilities. *Science* **133**(3466), 1749–1757. https://doi.org/10.1126/science.133.3466.1749 (1961).

2. Strother, L., Zhou, Z., Coros, A. K. & Vilis, T. An fMRI study of visual Hemifield integration and cerebral lateralization. *Neuropsychologia* **100**, 35–43. https://doi.org/10.1016/j.neuropsychologia.2017.04.003 (2017).
3. Goodale, M. A. & Milner, D. A. Separate visual pathways for perception and action. *Trends Neurosci.* **15**(1), 20–25. https://doi.org/10.1016/0166-2236(92)90344-8 (1992).
4. Ungerleider, L. G. & Mishkin, M. Two cortical visual systems. In *Analysis of Visual Behavior* (eds Ingle, D. J., Goodale, M. A. & Masfield, R. J. W.) 549–586 (MIT Press, 1982).
5. Prime, S. L., Vesia, M., & Crawford, J. D. Transcranial magnetic stimulation over posterior parietal cortex disrupts transsaccadic memory of multiple objects. *J. Neurosci.* **28**(27), 6938-6949. https://doi.org/10.1523/JNEUROSCI.0542-08 (2008).
6. Medendorp, W. P., Goltz, H. C., Vilis, T., & Crawford, J. D. Eye-centered remapping of remembered visual space in human parietal cortex. *J. Vis.* **3**(9), 125-125. https://doi.org/10.1167/3.9.125 (2003).
7. Merriam, E. P., Genovese, C. R. & Colby, C. L. Spatial updating in human parietal cortex. *Neuron* **39**(2), 361–373. https://doi.org/10.1016/S0896-6273(03)00393-3 (2003).
8. Sereno, M. I., Pitzalis, S. & Martinez, A. Mapping of contralateral space in retinotopic coordinates by a parietal cortical area in humans. *Science* **294**(5545), 1350–1354. https://doi.org/10.1126/science.1063695 (2001).
9. Mooshagian, E., Yttri, E. A., Loewy, A. D. & Snyder, L. H. Contralateral limb specificity for movement preparation in the parietal reach region. *J. Neurosci.* **42**(9), 1692–1701. https://doi.org/10.1523/JNEUROSCI.0232-21.2021 (2022).
10. Goodale, M. A. & Westwood, D. A. An evolving view of duplex vision: separate but interacting cortical pathways for perception and action. *Curr. Opin. Neurobiol.* **14**(2), 203–211. https://doi.org/10.1016/j.conb.2004.03.002 (2004).
11. Milner, D. A. & Goodale, M. A. Two visual systems re-viewed. *Neuropsychologia* **46**(3), 774–785. https://doi.org/10.1016/j.neuropsychologia.2007.10.005 (2008).
12. Milner, D. A. How do the two visual streams interact with each other? *Exp. Brain Res.* **235**(5), 1297–1308. https://doi.org/10.1007/s00221-017-4917-4 (2017).
13. Grill-Spector, K., Kourtzi, Z. & Kanwisher, N. The lateral occipital complex and its role in object recognition. *Vision. Res.* **41**(10–11), 1409–1422. https://doi.org/10.1016/S0042-6989(01)00073-6 (2001).
14. Kanwisher, N., Chun, M. M., McDermott, J. & Ledden, P. J. Functional imaging of human visual recognition. *Cogn. Brain. Res.* **5**(1–2), 55–67. https://doi.org/10.1016/S0926-6410(96)00041-9 (1996).
15. Hagler, D. J., Riecke, L. & Sereno, M. I. Parietal and superior frontal visuospatial maps activated by pointing and saccades. *NeuroImage* **35**(4), 1562–1577. https://doi.org/10.1016/j.neuroimage.2007.01.033 (2007).
16. Levy, I., Schluppeck, D., Heeger, D. J. & Glimcher, P. W. Specificity of human cortical areas for reaches and saccades. *J. Neurosci.* **27**(17), 4687–4696. https://doi.org/10.1523/JNEUROSCI.0459-07.2007 (2007).
17. Vesia, M. & Crawford, J. D. Specialization of reach function in human posterior parietal cortex. *Exp. Brain Res.* **221**(1), 1–18. https://doi.org/10.1007/s00221-012-3158-9 (2012).
18. Crawford, J. D., Henriques, D. Y. P. & Medendorp, W. P. Three-dimensional transformations for goal-directed action. *Annu. Rev. Neurosci.* **34**, 309–331. https://doi.org/10.1146/annurev-neuro-061010-113749 (2011).
19. Gaymard, B., Ploner, C. J., Rivaud, S., Vermersch, A. I. & Pierrot-Deseilligny, C. Cortical control of saccades. *Exp. Brain Res.* **123**(1–2), 159–163. https://doi.org/10.1007/s002210050557 (1998).
20. Lynch, J. C. & Tian, J. R. Cortico-cortical networks and cortico-subcortical loops for the higher control of eye movements. *Prog. Brain Res.* **151**, 461–501. https://doi.org/10.1016/S0079-6123(05)51015-X (2006).
21. Astafiev, S. V. et al. Functional organization of human intraparietal and frontal cortex for attending, looking, and pointing. *J. Neurosci.* **23**(11), 4689–4699. https://doi.org/10.1523/jneurosci.23-11-04689.2003 (2003).
22. Farrant, K. & Uddin, L. Q. Asymmetric development of dorsal and ventral attention networks in the human brain. *Dev. Cogn. Neurosci.* **12**, 165–174. https://doi.org/10.1016/j.dcn.2015.02.001 (2015).
23. Fox, M. D., Corbetta, M., Snyder, A. Z., Vincent, J. L. & Raichle, M. E. Spontaneous neuronal activity distinguishes human dorsal and ventral attention systems. *Proc. Natl. Acad. Sci. U.S.A.* **103**(26), 10046–10051. https://doi.org/10.1073/pnas.0604187103 (2006).
24. Melcher, D. & Colby, C. L. Trans-saccadic perception. *Trends Cogn. Sci.* **12**(12), 466–473. https://doi.org/10.1016/j.tics.2008.09.003 (2008).
25. Prime, S. L., Tsotsos, L., Keith, G. P. & Crawford, J. D. Visual memory capacity in transsaccadic integration. *Exp. Brain Res.* **180**(4), 609–628. https://doi.org/10.1007/s00221-007-0885-4 (2007).
26. Tas, A. C., Moore, C. M. & Hollingworth An object-mediated updating account of insensitivity to transsaccadic change. *J. Vis.* **12**(11), 18–18. https://doi.org/10.1167/12.11.18 (2012).
27. Edwards, G., VanRullen, R. & Cavanagh, P. Decoding trans-saccadic memory. *J. Neurosci.* **38**(5), 1114–1123. https://doi.org/10.1523/JNEUROSCI.0854-17.2017 (2018).
28. Prime, S. L., Vesia, M. & Crawford, J. D. Cortical mechanisms for trans-saccadic memory and integration of multiple object features. *Philos. Trans. R. Soc. B: Biol. Sci.* **366**(1564), 540–553. https://doi.org/10.1098/rstb.2010.0184 (2011).
29. Baltaretu, B. R., Monaco, S., Velji-Ibrahim, J., Luabeya, G. N. & Crawford, J. D. Parietal cortex integrates object orientation and saccade signals to update Grasp plans. *J. Neurosci.* **40**(23), 4525–4535. https://doi.org/10.1101/758532 (2020).
30. Baltaretu, B. R., Dunkley, B. T., Stevens, W. D. & Crawford, J. D. Occipital cortex is modulated by transsaccadic changes in spatial frequency: An fMRI study. *Sci. Rep.* **11**(1), 1–14. https://doi.org/10.1038/s41598-021-87506-2 (2021).
31. Dunkley, B. T., Baltaretu, B. R. & Crawford, J. D. Trans-saccadic interactions in human parietal and occipital cortex during the retention and comparison of object orientation. *Cortex* **82**, 263–276. https://doi.org/10.1016/j.cortex.2016.06.012 (2016).
32. Malik, P., Dessing, J. C. & Crawford, J. D. Role of early visual cortex in trans-saccadic memory of object features. *J. Vis.* **15**(11), 1–17. https://doi.org/10.1167/15.11.7.doi (2015).
33. Merriam, E. P., Genovese, C. R. & Colby, C. L. Remapping in human visual cortex. *J. Neurophysiol.* **97**(2), 1738–1755. https://doi.org/10.1152/jn.00189.2006 (2007).
34. Berman, R. A. & Colby, C. L. Attention and active vision. *Vis. Res.* **49**(10), 1233–1248. https://doi.org/10.1016/j.visres.2008.06.017 (2009).
35. Friston, K. J. Functional and effective connectivity in neuroimaging: A synthesis. *Hum. Brain. Mapp.* **2**, 56–78. https://doi.org/10.1002/hbm.460020107 (1994).
36. Engel, A. K., Fries, P. & Singer, W. Dynamic predictions: oscillations and synchrony in top–down processing. *Nat. Rev. Neurosci.* **2**(10), 704–716. https://doi.org/10.1038/35094565 (2001).
37. Buschman, J. et al. Synchronous oscillatory neural ensembles for rules in the prefrontal cortex. *Neuron* **76**(4), 838–846. https://doi.org/10.1016/j.neuron.2012.09.029 (2012).
38. de Pasquale, F. et al. A cortical core for dynamic integration of functional networks in the resting human brain. *Neuron* **74**(4), 753–764. https://doi.org/10.1016/j.neuron.2012.03.031 (2012).
39. Baltaretu, B. R., Stevens, W. D., Freud, E. & Crawford, J. D. Occipital and parietal cortex participate in a cortical network for transsaccadic discrimination of object shape and orientation. *Sci. Rep.* **13**(1), 11628. https://doi.org/10.1038/s41598-023-38554-3 (2023).
40. Ghaderi, A., Niemeier, M. & Crawford, J. D. Saccades and presaccadic stimulus repetition alter cortical network topology and dynamics: evidence from EEG and graph theoretical analysis. *Cereb. Cortex* **33**(5), 2075–2100. https://doi.org/10.1093/cercor/bhac194 (2023a).

41. Rubinov, M. & Sporns, O. Complex network measures of brain connectivity: uses and interpretations. *NeuroImage* **52**(3), 1059–1069. https://doi.org/10.1016/j.neuroimage.2009.10.003 (2010).
42. Boccaletti, S., Latora, V., Moreno, Y., Chavez, M. & Hwang, D. U. Complex networks: Structure and dynamics. *Phys. Rep.* **424**(4–5), 175–308. https://doi.org/10.1016/j.physrep.2005.10.009 (2006).
43. Bullmore, E. & Sporns, O. Complex brain networks: graph theoretical analysis of structural and functional systems. *Nat. Rev. Neurosci.* **10**(3), 186–198. https://doi.org/10.1038/nrn2575 (2009).
44. Newman, M. Fast algorithm for detecting community structure in networks. *Phys. Rev. E* **69**(6). https://doi.org/10.1103/PhysRevE.69.066133 (2004).
45. Rubinov, M. & Sporns, O. Weight-conserving characterization of complex functional brain networks. *NeuroImage* **56**(4), 2068–2079. https://doi.org/10.1016/j.neuroimage.2011.03.069 (2011).
46. Reavis, E. A. et al. Structural and functional connectivity of visual cortex in schizophrenia and bipolar disorder: A Graph-theoretic analysis. *Schizophrenia Bull. Open.* **1**(1). https://doi.org/10.1093/schizbullopen/sgaa056 (2020).
47. Stevens, W. D., Buckner, R. L. & Schacter, D. L. Correlated low-frequency BOLD fluctuations in the resting human brain are modulated by recent experience in category-preferential visual regions. *Cereb. Cortex* **20** (8), 1997–2006. https://doi.org/10.1093/cercor/bhp270 (2010).
48. Wang, L., Mruczek, R. E. B., Arcaro, M. J. & Kastner, S. Probabilistic maps of visual topography in human cortex. *Cereb. Cortex.* **25**(10), 3911–3931. https://doi.org/10.1093/cercor/bhu277 (2015).
49. Newman, M. Modularity and community structure in networks. *Proc. Natl. Acad. Sci.* **103**(23), 8577–8582. https://doi.org/10.1073/pnas.0601602103 (2006).
50. Avena-Koenigsberger, A., Misic, B. & Sporns, O. Communication dynamics in complex brain networks. *Nat. Rev. Neurosci.* **19**(1), 17–33. https://doi.org/10.1038/nrn.2017.149 (2017).
51. Curtis, C. E. & D'Esposito, M. Persistent activity in the prefrontal cortex during working memory. *Trends Cogn. Sci.* **7**(9), 415–423. https://doi.org/10.1016/S1364-6613(03)00197-9 (2003).
52. Prime, S. L., Vesia, M. & Crawford, J. D. TMS over human frontal eye fields disrupts trans-saccadic memory of multiple objects. *Cereb. Cortex* **20**(4), 759–772. https://doi.org/10.1093/cercor/bhp148 (2010).
53. Barash, S., Bracewell, R. M., Fogassi, L., Gnadt, J. W. & Andersen, R. A. Saccade-related activity in the lateral intraparietal area. II. Spatial properties. *J. Neurophysiol.* **66**(3), 1109–1124. https://doi.org/10.1152/jn.1991.66.3.1109 (1991).
54. Grefkes, C. & Fink, G. R. The functional organization of the intraparietal sulcus in humans and monkeys. *J. Anat.* **207**(1), 3–17. https://doi.org/10.1111/j.1469-7580.2005.00426.x (2005).
55. Aminoff, E. M., Kveraga, K. & Bar, M. The role of the parahippocampal cortex in cognition. *Trends Cogn. Sci.* **17**(8), 379–390. https://doi.org/10.1016/j.tics.2013.06.009 (2013).
56. Grill-Spector, K. et al. Differential processing of objects under various viewing conditions in the human lateral occipital complex. *Neuron* **24**(1), 187–203. https://doi.org/10.1016/S0896-6273(00)80832-6 (1999).
57. Bassett, D. S., Brown, J. A., Deshpande, V., Carlson, J. M. & Grafton, S. T. Conserved and variable architecture of human white matter connectivity. *NeuroImage* **54**(2), 1262–1279. https://doi.org/10.1016/j.neuroimage.2010.09.006 (2011).
58. de Reus, M. A. & van den Heuvel, M. P. The parcellation-based connectome: Limitations and extensions. *NeuroImage* **80**, 397–404. https://doi.org/10.1016/j.neuroimage.2013.03.053 (2013).
59. Zalesky, A. et al. Whole-brain anatomical networks: Does the choice of nodes matter? *NeuroImage* **50**(3), 970–983. https://doi.org/10.1016/j.neuroimage.2009.12.027 (2010).
60. van Wijk, B. C. M., Stam, C. J. & Daffertshofer, A. Comparing brain networks of different size and connectivity density using graph theory. *PLoS ONE* **5**(10). https://doi.org/10.1371/journal.pone.0013701 (2010).
61. Fornito, A., Zalesky, A. & Bullmore, E. T. Network scaling effects in graph analytic studies of human resting-state fMRI data. *Front. Syst. Neurosci.* **4**, 22. https://doi.org/10.3389/fnsys.2010.00022 (2010).
62. Chong, M. et al. Individual parcellation of resting fMRI with a group functional connectivity prior. *NeuroImage* **156**, 87–100. https://doi.org/10.1016/j.neuroimage.2017.04.054 (2017).
63. Yu, Q. et al. Application of graph theory to assess static and dynamic brain connectivity: Approaches for building brain graphs. *Proc. IEEE* **106**(5), 886–906. (2018). https://doi.org/10.1109/JPROC.2018.2825200
64. Pisella, L., Binkofski, F., Lasek, K., Toni, I. & Rossetti, Y. No double-dissociation between optic ataxia and visual agnosia: multiple sub-streams for multiple visuo-manual integrations. *Neuropsychologia* **44**(13), 2734–2748. https://doi.org/10.1016/j.neuropsychologia.2006.03.027 (2006).
65. Rossetti, Y., Pisella, L. & McIntosh, R. D. Rise and fall of the two visual systems theory. *Annals Phys. Rehab. Med.* **60**(3), 130–140. https://doi.org/10.1016/j.rehab.2017.02.002 (2017).
66. Schenk, T. & McIntosh, R. D. Do we have independent visual streams for perception and action? *Cogn. Neurosci.* **1**(1), 52–62. https://doi.org/10.1080/17588920903388950 (2010).
67. Chen, Y. et al. Allocentric versus egocentric representation of remembered reach targets in human cortex. *J. Neurosci.* **34**(37), 12515–12526. https://doi.org/10.1523/JNEUROSCI.1445-14.2014 (2014).
68. Rolfs, M. & Carrasco, M. Rapid simultaneous enhancement of visual sensitivity and perceived contrast during saccade preparation. *J. Neurosci.* **34**(40), 13744–11375. https://doi.org/10.1523/JNEUROSCI.2676-12.2012 (2012).
69. White, A. L., Rolfs, M. & Carrasco, M. Adaptive deployment of Spatial and feature-based attention before saccades vision research. **85**, 26–35. https://doi.org/10.1016/j.visres.2012.10.017 (2013).
70. Golomb, J. D. Remapping locations and features across saccades: a dual-spotlight theory of attentional updating. *Curr. Opin. Psychol.* **29**, 211–218. https://doi.org/10.1016/j.copsyc.2019.03.018 (2019).
71. Corbetta, M. & Shulman, G. L. Control of goal-directed and stimulus-driven attention in the brain. *Nat. Rev. Neurosci.* **3**(3), 201–215. https://doi.org/10.1038/nrn755 (2002).
72. Jerde, T. A., Merriam, E. P., Riggall, A. C., Hedges, J. H. & Curtis, C. E. Prioritized maps of space in human frontoparietal cortex. *J. Neurosci.* **32**(48), 17382–17390. https://doi.org/10.1523/JNEUROSCI.3810-12.2012 (2012).
73. Silver, M. A. & Kastner, S. Topographic maps in human frontal and parietal cortex. *Trends Cogn. Sci.* **13**(11), 488–495. https://doi.org/10.1016/j.tics.2009.08.005 (2009).
74. Vossel, S., Geng, J. J. & Fink, G. R. Dorsal and ventral attention systems: Distinct neural circuits but collaborative roles. *Neuroscientist* **20**(2), 150–159. https://doi.org/10.1177/1073858413494269 (2014).
75. Corbetta, M., Kincade, M. J., Lewis, C., Snyder, A. Z. & Sapir, A. Neural basis and recovery of spatial attention deficits in spatial neglect. *Nat. Neurosci.* **8**(11), 1603–1610. https://doi.org/10.1038/nn1574 (2005).
76. Karnath, H. O., Ferber, S. & Himmelbach, M. Spatial awareness is a function of the temporal not the posterior parietal lobe. *Nature* **411**(6840), 950–953. https://doi.org/10.1038/35082075 (2001).
77. Mort, D. J. et al. The anatomy of visual neglect. *Brain* **126**(9), 1986–1997. https://doi.org/10.1093/brain/awg200 (2003).
78. Logothetis, N., Pauls, J., Augath, M., Trinath, T. & Oeltermann, A. Neurophysiological investigation of the basis of the fMRI signal. *Nature* **412**, 150–157. https://doi.org/10.1038/35084005 (2001).
79. Corbetta, M., Patel, G. & Shulman, G. L. The reorienting system of the human brain: From environment to theory of Mind. *Neuron* **58**(3), 306–324. https://doi.org/10.1016/j.neuron.2008.04.017 (2008).
80. Crespi, S. et al. Spatiotopic coding of BOLD signal in human visual cortex depends on Spatial attention. *PloS One* **6**(7), e21661. https://doi.org/10.1371/journal.pone.0021661 (2011).

81. Ghaderi, A., Niemeier, M. & Crawford, J. D. Saccades alter cortical network modularity and decrease lateralization in a visual perception task. *J. Vis.* **23**(9), 5510. https://doi.org/10.1167/jov.23.9.5510 (2023b).
82. Wang, R. F. et al. Spatial updating relies on an egocentric representation of space: effects of the number of objects. *Psychonomic Bull. Rev.* **13**, 281–286. https://doi.org/10.3758/BF03193844 (2006).
83. Sommer, M. A. & Wurtz, R. H. Brain circuits for the internal monitoring of movements. *Annu. Rev. Neurosci.* **31**, 317–338. https://doi.org/10.1146/annurev.neuro.31.060407.125627 (2008).
84. Fabius, J., Fracasso, A., Deodato, M. & Melcher, D. Bilateral increase in MEG planar gradients prior to saccade onset. *Sci. Rep.* **13**(1). https://doi.org/10.1038/s41598-023-32980-z (2023).
85. Tanaka, L., Dessing, J. J., Malik, P., Prime, S. L. & Crawford, J. D. The effects of TMS over dorsolateral prefrontal cortex on trans-saccadic memory of multiple objects. *Neuropsychologia* **63**, 185–193. https://doi.org/10.1016/j.neuropsychologia.2014.08.025 (2014).
86. Press, W. A., Brewer, A. A., Dougherty, R. F., Wade, A. R. & Wandell, B. A. Visual areas and spatial summation in human visual cortex. *Vis. Res.* **41**(10–11), 1321–1332. https://doi.org/10.1016/S0042-6989(01)00074-8 (2001).
87. Arcaro, M. J. & Kastner, S. Topographic organization of areas V3 and V4 and its relation to supra-areal organization of the primate visual system. *Vis. Neurosci.* **23**(11). https://doi.org/10.1017/S0952523815000115 (2015).
88. Bressler, S. L., Tang, W., Sylvester, C. M., Shulman, G. L. & Corbetta, M. Top-down control of human visual cortex by frontal and parietal cortex in anticipatory visual spatial attention. *J. Neurosci.* **28**(40), 10056–10061. https://doi.org/10.1523/JNEUROSCI.1776-08.2008 (2008).
89. Faul, F., Erdfelder, E., Buchner, A. & Lang, A. G. Statistical power analyses using G*Power 3.1: Tests for correlation and regression analyses. *Behav. Res. Methods* **41**(4), 1149–1160. https://doi.org/10.3758/BRM.41.4.1149 (2009).
90. Talairach, J., Rayport, M. & Tournoux, P. *Co-Planar Stereotaxis Atlas of the Human Brain: an Approach To Cerebral Imaging* (Thieme, 1988).
91. Watts, D. J. & Strogatz, S. H. Collective dynamics of small-world networks. *Nature* **393**(6684), 440–442. https://doi.org/10.1038/30918 (1998).
92. Latora, V. & Marchiori, M. Efficient behavior of small-world networks. *Phys. Rev. Lett.* **87**(19). https://doi.org/10.1103/PhysRevLett.87.198701 (2001).
93. Nichols, T. E. & Holmes, A. P. Nonparametric permutation tests for functional neuroimaging: A primer with examples. *Hum. Brain. Mapp.* **15**(1), 1–25. https://doi.org/10.1002/hbm.1058 (2001).
94. Benjamini, Y. & Yekutieli, D. False discovery rate-adjusted multiple confidence intervals for selected parameters. *J. Am. Stat. Assoc.* **100**(469), 71–81. https://doi.org/10.1198/016214504000001907 (2005).
95. Groppe, D. M., Urbach, T. P. & Kutas, M. Mass univariate analysis of event-related brain potentials/fields I: A critical tutorial review. *Psychophysiology* **48**(12), 1711–1725. https://doi.org/10.1111/j.1469-8986.2011.01273.x (2011).
96. Xia, M., Wang, J. & He, Y. BrainNet viewer: A network visualization tool for human brain connectomics. *PLoS ONE* **8**, e68910. https://doi.org/10.1371/journal.pone.0068910 (2013).

Acknowledgements

The authors thank S. Sun, Xiaogang Yan, and Diana Gorbet for technical assistance. This research was supported by the Natural Science and Engineering Research Council of Canada. G.T. and A.G. were supported by the Vision: Science to applications program, funded in part by the Canada First Research Excellence Fund. G.T. was also supported by an Ontario Graduate Scholarship (OGS). B.B. was supported by an OGS / Queen Elizabeth II Graduate Scholarship in Science and Technology. J.D.C. was supported by a York Research Chair.

Author contributions

G.T. performed the graph theory analysis and wrote the manuscript. B.R.B. recorded and preprocessed the data and reviewed the paper. A.G. supervised the graph theory analysis and edited the original manuscript. J.D.C conceived and supervised the study, provided resources, and edited the manuscript.

Declarations

Competing interests

The authors declare no competing interests.

Additional information

Supplementary Information The online version contains supplementary material available at https://doi.org/10.1038/s41598-025-95568-9.

Correspondence and requests for materials should be addressed to J.D.C.